AUBURN UNIVERSITY
FOREST HEALTH COOPERATIVE

RESEARCH REPORT 19-05

IDENTIFYING FUNGAL SPORES ON COLEOPTERA
WITH HYPERSPECTRAL INTERFEROMETRY

by
Jessica Ahl and Lori Eckhardt

3.1. ABSTRACT

Previous work with hyperspectral interferometry on bark beetles revealed oscillatory signals from specific surface features. Best resembling an interference pattern as from a Fabry- Perot model, this instance is unique in that the etalon is produced outside of the microscope measuring system and is instead on the surface feature being observed. Setae and spore-like objects on the beetle were described, with further work here being given to spores. Here, *Hylastes salebrosus* beetles were used as surfaces to detect spores of three different species. For us, the reflecting surface was the spore, outside the microscope measuring system, which had two or more surfaces. This pilot study determined whether interferometry could differentiate spore type on a beetle surface. Sizes and power spectra were obtained from spores, and maps of spores as they laid out on the beetles' surface were created with the use of a computer program in ImageJ. Statistical analysis revealed that two out of three fungal species could be differentiated with hyperspectral interferometry. However, two species had close average means and are likely not capable of being distinguished from one another in this manner.

3.2. INTRODUCTION

Previous work with hyperspectral imaging has centered on fields in medicine, pharmacy, agriculture, and astronomy (Hege et al. 2003; Rodionova et al. 2005; Del Fiore et al. 2010; More et al. 2016). While previous work by Beach et al. (2015) showed a capability of observing and sizing spores on bark beetles, further research is needed to determine if it is possible to speciate spores using this method. Current methods of fungal identification involve culturing samples on media plates, often utilizing time periods of three weeks or more, and using molecular analyses such as PCR and DNA fingerprinting (Six et al. 2003). Additional studies could provide a quicker and more cost efficient alternative to fungal identification, quickening management implementation.

As phytophagous insects, *H. salebrosus* feed on pine roots and stumps, and have even been documented on green seedlings (Wood 1982). These beetles are known carriers of ophiostomatoid fungi such as *Leptographium* and *Grosmannia* (Klepzig et al. 1991, Jacobs and Wingfield 2001; Matusick et al. 2013) that cause blue staining and vascular occlusion of wood tissues (Eckhardt et al. 2007). These effects can be detrimental to the forestry industry, as they devalue wood and affect tree growth (Rane and Tattar, 1987; Eckhardt et al. 2004a). Other fungal species, including yeasts and *Graphium*, have also been found associated with *Hylastes* species (Dowding 1973; Wingfield and Gibbs 1991) and add to the ecology of microflora found on these beetles.

In bark beetles, including *Hylastes*, fungi are often vectored externally on beetle surfaces, internally through the digestive system, and sometimes in specialized body structures called mycangia (Harrington 1993). These ophiostomatoid fungi have spores that are coated and sticky, allowing for adherence to the insect body. Whitney and Blauel (1972) suggested this was to prevent washing off by rain and instead allows for detachment in resin filled galleries of new dispersal trees. In addition to this, the mucilage allows for spores to travel as discrete masses and keeps them moist (Dowding 1969) and in some species, can allow for safe gastrointestinal travel (Francke-Grosmann 1963). Furthermore, fungal spores have been collected by rolling *Hylastes salebrosus* beetles over media plates, lending additional support to the idea that these spores are vectored externally in this species (Eckhardt et al. 2007).

Here, we observed spores of three species in an attempt to differentiate them: *Grosmannia alacris* T.A. Duong, Z.W. de beer & M.J. Wingf., *Leptographium procerum*, and a *Graphium* species. *Grosmannia alacris* has spores that are hyaline, aseptate, and oblong with rounded apices and truncate bases. The fungi are reported to have spores in the size range of (4.5-)5.1-6.1(-6.8) X (1.8-)2.1-2.4(-2.6) µm, depending on genetics and environmental conditions (Duong et al. 2012). Likewise, *L. procerum* has spores with a similar shape, ranging from hyaline, aseptate, obovoid to broadly ellipsoid with rounded apices and truncate bases.

Their sizes range from (3 – 5) x (1 – 3) µm (Jacobs and Wingfield 2001). In addition to these known pathogenic species, we also looked at an unknown *Graphium* species that is also carried by *Hylastes* as a comparison. Spores from this fungus measured between (0.6 – 1.1) x (0.7 – 1.2) µm within the mucilage covering, as observed within this study.

3.3. MATERIALS AND METHODS

3.3.1. Site Location

Spore preparation was done in the laboratory at the Forest Health Cooperative at Auburn University in Auburn, AL. Hyperspectral imaging of both spores and beetles was done at CytoViva, Inc. in Auburn, AL.

3.3.2 Fungal spore cultures and observation

Fungal cultures each of *L. procerum* and *G. alacris* were used from the existing culture collection at the Forest Health Cooperative Laboratory at Auburn University. Fungi were cultured on media plates composed of twice sterilized loblolly pine (*Pinus taeda*) twigs and 1% malt extract agar. Plates of oatmeal agar were used to encourage sporulation of difficult or slow to sporulate species such as *L. procerum*. Cultures were allowed to grow for 14 days inside an incubator at 25 °C.

Fungal smears on microscope slides were initially obtained by sterile technique onto empty 75x25x1 mm microscope slides (VWR VistaVision). Microscope slides were fitted with an o-ring (Danco, #15, 1x0.75x0.125 in.) sealed in place with clear nail polish (Sally Hansen, Hard as Nails, 0.45 fl. oz.) (Fig. 3.1). Spores were smeared inside the o-ring, next to an adjacent drop of distilled water and covered with an 18x18 mm, 1 oz. cover glass (Fisher Scientific, Pittsburgh, PA) to preserve humidity until observation. Prepared slides were then placed onto a napkin damp with distilled water inside a sterilized empty 28.5 oz. plastic container with a lid (Breyers Ice Cream) for transport to CytoViva, Inc.

However, as our ultimate goal was to obtain readings directly from beetle surfaces, wesought another object similar glass slides as an alternative. The reflective nature of clear glass proved to be an interference in initial results, so to reduce interference from strong light reflections produced by the clear microscope slide, fungal species were subsequently observed on black glass seed beads (Cousin, 1.41. oz.) (Fig. 3.2). This was done by sterilizing beads in 95% alcohol for 30 seconds and allowing them to dry before rolling beads on sporulating plates of fungi. Beads were then placed onto sterilized 3" x 1" concavity microscope slides (Ted Pella, Inc., 1-1.2 mm wide) for observation.

3.3.3. Beetle Trapping and Preparation

Hylastes salebrosus beetles were captured with the use of both ground based panel traps and hanging panel traps placed at Auburn University's Mary Olive Thomas Demonstration Forest and the Louise Kreher Forest Ecology Preserve in Auburn, Alabama from February through June 2018. Pitfalls consisted of a 20-cm length of a 10-cm diameter polyvinyl chloride plastic pipe with eight holes spaced equally around the circumference (Klepzig et al. 1991) (Fig. 3.3). Both ends of the pipe had caps that served as removable lids, with holes drilled into the bottom cap for drainage. Traps were buried into the soil and leaf litter until the entrance holes lined up at ground level. These traps' interiors were coated with a layer of liquid Teflon^{TM} (Northern Products Woonsockets, RI) to prevent insects from climbing out once inside. Panel traps (APTIV Company, Portland, Oregon) made of black corrugated plastic and Lindgren were funnels hung on metal poles one meter above the ground and had a plastic cup attached to the bottom to capture flying beetles (Fig. 3.4).

Both trap types included two 8 mL glass vials hung and filled with 90% 3-carene (Sigma-Aldrich) and 95% ethanol (1:1), respectively. These acted as an attractant to obtain more *Hylastes* over other bark beetles (Kelsey and Westlind 2018). Traps were checked and vials refilled every three days during the collection period. After identification, captured *Hylastes salebrosus* were put into the cooler at 4 ºC to keep fresh until use and were utilized within 30 days of capture.

Beetle preparation involved washing *H. salebrosus* in 95% ethanol (Beach et al. 2015) for 30 seconds and allowing them to dry. Specimens were then rolled onto sporulating fungal plates with the use of sterilized forceps. Beetles were then transported to CytoViva inside of sterilized 2 oz. condiment cups (Dixie), Inc. for microscopic imaging on concavity microscope slides.

3.3.4. Reflected Light Microscopy

An upright microscope (Olympus BX-43) was used to observe beetles at 10X magnification with bright-field reflected light. Focus was used to examine areas and to obtain discernable, quality images of surface features on the beetles. Illumination was provided by a lamp using a halogen source and aluminized reflectors to provide a spectral range of visible and near infrared

wavelengths. To direct light at the specimen and provide illumination, a half-silver mirror was used, passing reflected light to a detector (Beach et al. 2015).

3.3.5 Hyperspectral Imaging

The CytoViva hyperspectral imaging system uses a motorized stage to move a sample over a set scale of small distances, allowing for a camera to take pictures every time the stage stops. The camera is spectrographic, capable of capturing visible near-infrared (VIS-NIR) images; it comprises of an imaging spectrograph and a CCD camera and mounted to the imaging port of the microscope. Two spatial dimensions, X and Y, are used in a grid-coordinate system. A motion algorithm guides the movement of the stage, making it equivalent to the pixel spacing along X and projecting correct image geometry. The spatial resolution for the microscope at 10X objective magnification is 1.29 μm.

3.3.6 Size Estimation and Spectral Analysis of Spore Size

Oscillations of spore spectra were taken from spectra in hyperspectral images using Z axis profiles of associated pixels. The separation between adjacent intensity maxima or minima in the oscillations on single pixels were used to determine oscillation frequencies. Sizes were determined based on the assumption that oscillation waveforms came from the interference caused by multiple surface reflections. The surface oscillations were obtained in the form of maps with the use of ImageJ using the hyperspectral image.

The usage of the "Analyze Particles" feature in ImageJ also provided rough estimate of initial spore assessments, allowing for non-conforming pixels to be excluded out of these sizing procedures. The feature gave an output of average area in the form of image pixels; knowing pixel size, we were able to calculate average area. Detectable by a map later developed in ImageJ, these same objects allowed us to analyze the spectral oscillations and we compared these average area outputs to the sizes in the model. The closer both values were to each other, then the more supportive the results.

3.3.7 Etalon Modeling

As oscillations arise from interference produced by multiple surfaces, a semitransparent object like a spore provides a path for light between back and front surfaces, using the change in the refractive index to produce a reflection. A fraction of the light gets reflected back into the object, and a standing wave pattern is produced as light goes back and forth between surfaces. This effect is similar to the Fabry-Perot etalon model which uses two parallel surfaces. Beach et al. (2015) observed these spectra as a simple sine wave-like pattern, similar to the one produced by etalons in back-illuminated CCD image sensors. They explained the pattern as a product of the beetle spores' non-parallel surfaces. In addition to this, the exoskeleton scatters and absorbs light due to its lack of uniformity, adding to the less than optimum etalon production.

These method utilizes the space between pulses to determine size, and this space varies from point to point. Due to this, some averaging is required to utilize the etalon model (Beach et al. 2015). However, since we are only concerned with discovering the origin of the oscillations, the etalon model is fitting as it can determine the size of adhering spores.

Reflections straight off the beetle's surface are off a higher refractive index and return 180° degrees out-of-phase with the original light (Beach et al. 2015). The internal path is through a

higher refractive index, so reflections are from a high to low index and are therefore in phase. This final phase of reflection is determined as direct or indirect depending on the internal length of the light pathway and the optical wavelength. These reflections stay out of phase with each other, causing destructive interference and therefore reducing the light intensity, if there are a whole number of wavelengths to fill the pathway of the round trip. If the optical path difference is half an odd multiple of the wavelength then the reflections come into phase and increase the intensity. As a result, broadband illumination reflects as a function of wavelength, causing the reflected light spectrum' oscillations to appear between minimum and maximum values. This process is similar when the light passes through an object of lower refractive index, where the phase relationship is reversed but the oscillation period of the reflection spectrum is the same. The etalon free spectral range, defined by the separation between maxima, is equivalent to twice the number of wavelengths that go between the surfaces. The necessary number of optical waves, n, is determined by wavelengths of the two successive maxima by equating the conditions:

$$(n + 1)\lambda_{i-1} = n\lambda_i$$

$$= d$$

Here, λi-1 is the shorter wavelength maximum and λi is the next longer maximum. This function i defines a series of maxima with lengthening periods. As the wavelength increases, the oscillation frequencies decreases, following an inverse relationship. While this reflects an ideal situation, in actuality, the refractive index of the object is not constant across the wavelength and is obvious only if the range of the wavelengths is large. The number of roundtrip wavelengths with respect to wavelength λi is found by:

$$n = \lambda i\text{-}1(\lambda i - \lambda i\text{-}1)\text{-}1$$

$$= \lambda i\text{-}1\ vi$$

Here the oscillation frequency, vi takes the place of the reciprocal of the wavelength interval. The roundtrip distance through the object is also defined as:

$$d = 2\ \eta\ D\ \cos(\Theta)$$

Here, η is the refractive index, D is the distance between surfaces, and Θ is the angle of the light as it hits the surface. With regards to the nm range of 600 and 750, η is equivalent to 1.53 for fungal spores (Hart and Leski 2006) and 1.6 for chitin, the latter of which makes up the composition of insect exoskeletons (Azofeifa et al. 2012). Combining our first equation and this latest one for distance, we get:

$$D = n\ \lambda i\ (2\ \eta\ \cos(\Theta))\text{-}1$$

$$= \lambda i\text{-}1\ vi\ \lambda i\ (2\ \eta\ \cos(\Theta))\text{-}1$$

Assuming the cosine value is 1 (Beach et al. 2015), the latest equation represents the object dimension, defining it as proportional to the oscillation frequency between the two successive maxima. Given this, as long as η is known, this formula is valid over a wide range of

wavelengths. High frequencies correspond to large dimensions, while lower frequencies correspond to smaller dimensions. While the input of our model is the separation (nm) between adjacent peaks, the output is the value D. After converting to microns, this value serves as an estimate for the size of surface features.

Sampling error and background noise can affect results. Therefore, best values for maxima were determined by removing random noise with the use of a three-point moving average filter. The resulting wave then produced with frequency representing a linear function of wavelength.

3.3.8 Object Mapping by Fourier Analysis

Spore mapping was done with the use of the scientific image analysis program ImageJ. Similar to Beach et al. (2015), a code was generated for use after examining amplitudes of spores on slides and beads to map possible regions on spore loaded beetles while excluding non-spore features.

3.4. DATA ANALYSIS

Microscope captured images were analyzed with the ENVI 4.8 (Exelis Visual Information Solutions, Boulder, CO) program with features customized for microscopy (CytoViva, Auburn, AL). ImageJ was used to process data cube files and locate coordinates of interest. Spore sizes were calculated with the use of Excel 2016. SAS 9.4 was then used on compiled species' sizes to determine an analysis of variance. Paired species were then subsequently used in a T-test to determine if they could be differentiated.

3.5 RESULTS

Initial fungal smears on glass microscope slides produced observable spores at 100X magnification (Fig. 3.5) and associated wavelengths at certain coordinates on the edge of spores (Fig. 3.6). In Figure 3.5, the size of the selected spore at that coordinate was determined to be 1.583 μm when considering the two valleys in the wavelength, 449.75 and 495.11 nm, as per the model equation (Beach et al. 2015).

However, despite these results, additional reflectance from the clear glass slide used provided less than optimal waves, even if sizes were consistent. As the alternative, we turned to using glass seed beads which had the benefit of being black while fitting inside the microscope view piece. Spores also adhered easily to the sterilized bead surface and these were visible under the lens (Fig. 3.7). Similar to methods before, coordinates were located, wavelengths obtained, and sizes measured. In this way, we looked at spores of *Grosmannia alacris* and obtained wavelengths (Fig. 3.8).

To quicken spore region identification, we sought to develop a universal tool for use on images of beetle surfaces. Using initial amplitudes for spores we found, a code was generated for use in ImageJ to aid in locating spore areas on beetle surfaces. Named "FFT map" for its origin in the fast fourier transform method, ensuing images showed areas of potential for spores (Fig. 3.9). In addition to these images, our map code also produced an associated histogram and power spectrum for the overall image, the latter of which provided a relative measure through an index of frequencies, and which may provide an area for future study.

Beetles were spore loaded the same as beads and placed under the microscope. Values for each sample are listed in Table 3.1. The average results and p values from the one-tailed T tests are shown in Table 3.2. Two spore species – *G. alacris* and *L. procerum* – were significantly different in size from the others (F=7.07; P=0.0020; df=2; ANOVA; Fig. 3.10).

3.6 DISCUSSION

Oscillations in the spectrum of reflected light carries information about features on the surface of an object. Beach et al. (2015) showed that these features could be defined as diameters of clinging spores. We were able to observe spores in the visible and near-infrared range and deduce their size in methods replicable to the Fabry-Perot etalon model of their previous work. This work served as a pilot study for determining spore species based on hyperspectral interferometry. It was the first time interferometry has been used with the focus on spores and not only surface features of the beetle (Parker and Lawrence 2001; Galusha et al. 2008). Previous research has investigated insect colors as an impact of light reflection on body surfaces (Ghiradella 1991; Seago et al. 2009; Sharma et al. 2009) and the potential impacts on visual signaling (Shevtsova et al. 2011). Hyperspectral interferometry can identify fungal spores on the body of bark beetles to an extent, and our FFT map shows potential in identifying areas where spores can reside, however it needs much more automation. Bright spots for potential spore locations only showed up when the threshold value was just below the peak amplitude value. In addition to this, surface features such as setae can create etalons that are picked up on. A more universal, autonomous map should be developed, as this challenge is made more difficult by the fact that a beetle's surface provides more interference than a glass slide. This method could provide a simpler, optical technology for determining spore loads of beetles, aiding in an even quicker identification.

While we were able to observe spores on glass slides, getting consistent signatures from black, glass seed beads proved to be more successful, providing a concrete foundation for obtaining spore data on beetle surfaces. Our ANOVA and t tests results showed that we could differentiate two out of our three spore species with hyperspectral interferometry. However, *L. procerum* and *G. alacris* have close average mean sizes and likely cannot be discriminated on this alone. Data from our hyperspectral work (Fig. 3.10) supported previous measurements of *L. procerum* by Beach et al. (2015) and provided new data for *G. alacris* and the *Graphium* species through the use of hyperspectral interferometry. Our Graphium species' spores were shown to be smaller than the other two species, both in hyperspectral and manual methods. Differences in regards to this species' manual and hyperspectral methods may have resulted from the mucilage covering. Manual measurements were conservative where masses on beetles can be composed of many spores and mucilage. Additional areas of future research may focus on discerning differences in these coverings.

Considering the impact fungal carrying beetles can have on commercial forestation (Eckhardt et al., 2004a), these findings carry interest. Fungal identification can take weeks for samples to be collected and grown and for analyses such as DNA fingerprinting or PCR to be completed (Six et al., 2003). Further development in optical modeling and in hyperspectral techniques presented here and by Beach et al. (2015) may help to specify fungal spore identification and may have implications for other industries.

Table 3.1. Individual spore sizes recorded for each species using the hyperspectral method[a,b]

Species	***G. alacris***	***L. procerum***	***Graphium* sp.**
n	8	22	22
Sizes (µm)	2.7	3.86	1.97
	2.34	3.85	1.7
	2.2	3.12	3.22
	3.8	3	1.62
	2.68	3.2	3.19
	4.01	2.98	3.29
	3.34	2.67	1.92
	4.1	2.37	2.69
		2.56	1.88
		2.83	2.24
		3.69	1.53
		3.32	2.17
		2.85	2.5
		1.78	2.31
		1.9	2.84
		2.25	1.99
		3.06	1.77
		3.82	2.53
		1.78	2.22
		4.36	2.7
		4.56	1.84
		2.13	2.8

[a]Samples from single image pixels.

[b]Refractive index 1.53 is assumed.

Table 3.2. Fungal species *Grosmannia alacris* (GA), *Leptographium procerum* (LP), and the *Graphium* species (Gr), their documented sizes according to non-hyperspectral methods, our average size findings, and p values of t test results.

Species	**Documented sizes (µm)**	**N**	**Our Average Size (µm)**	**GA**	**LP**	**Gr**
GA	(4.5-6.8) x (1.8-2.6)	8	3.15	-		0.0011*
LP	(3-5) x (1-3)	22	3	0.325	-	0.00089*
Gr	(0.6-1.1) x (0.7-1.2)	22	2.31	0.0011*	0.00089*	-

*Significance

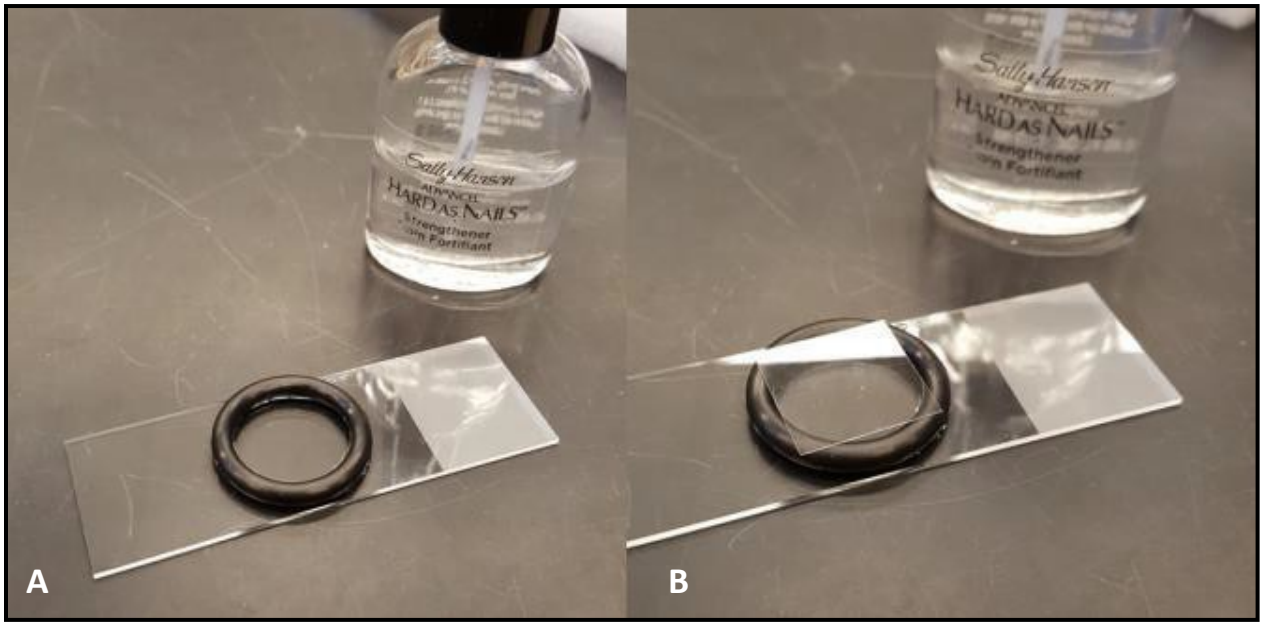

Figure 3.1. Microscope slides fitted with o-rings, (A) without a cover slip and (B) with a coverslip.

Figure 3.2. Glass seed beads (Cousin, 1.41 oz.) obtained for rolling onto spores.

Figure 3.3. A pitfall trap baited with hanging vials of 3- carene and 95% ethanol.

Figure 3.4. A panel trap to be baited with hanging vials of 3-carene and 95% ethanol.

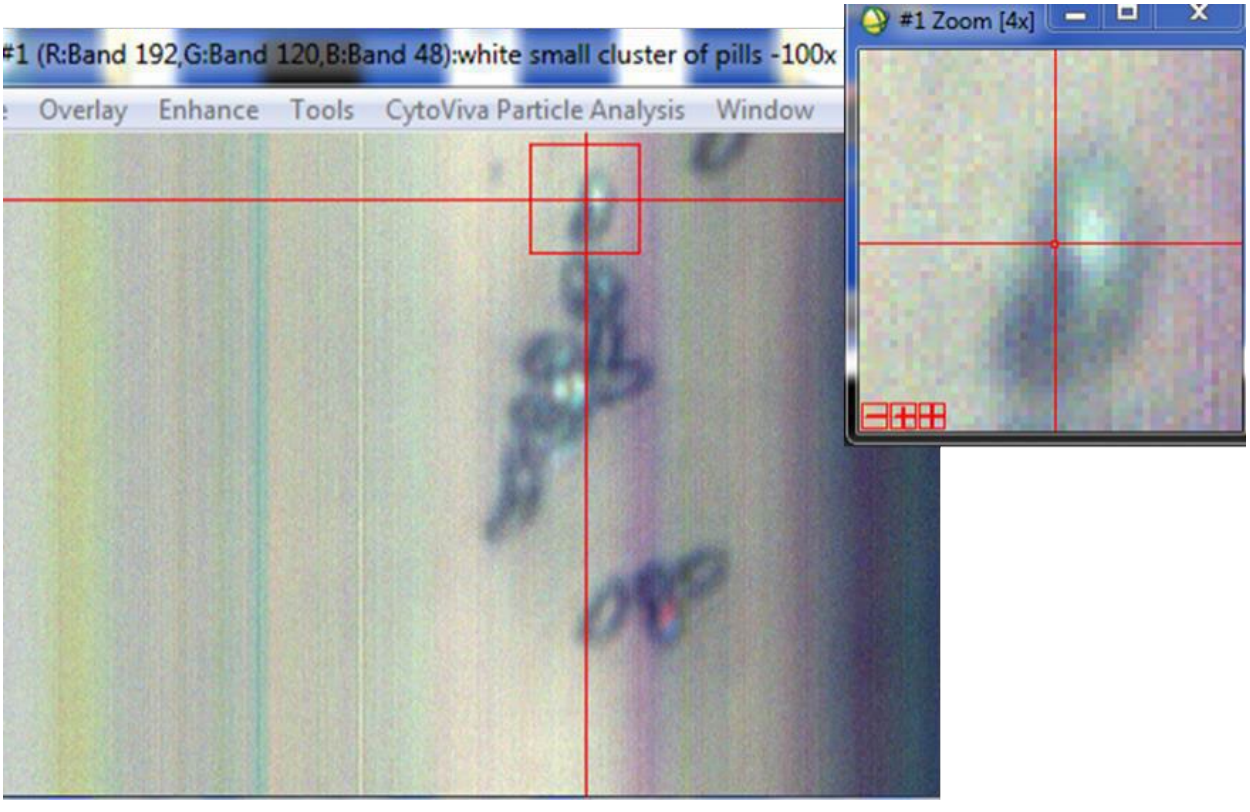

Figure 3.5. Spore smears of *Grosmannia alacris* on glass, viewed at 100X with a coordinate selected for the edge of a spore.

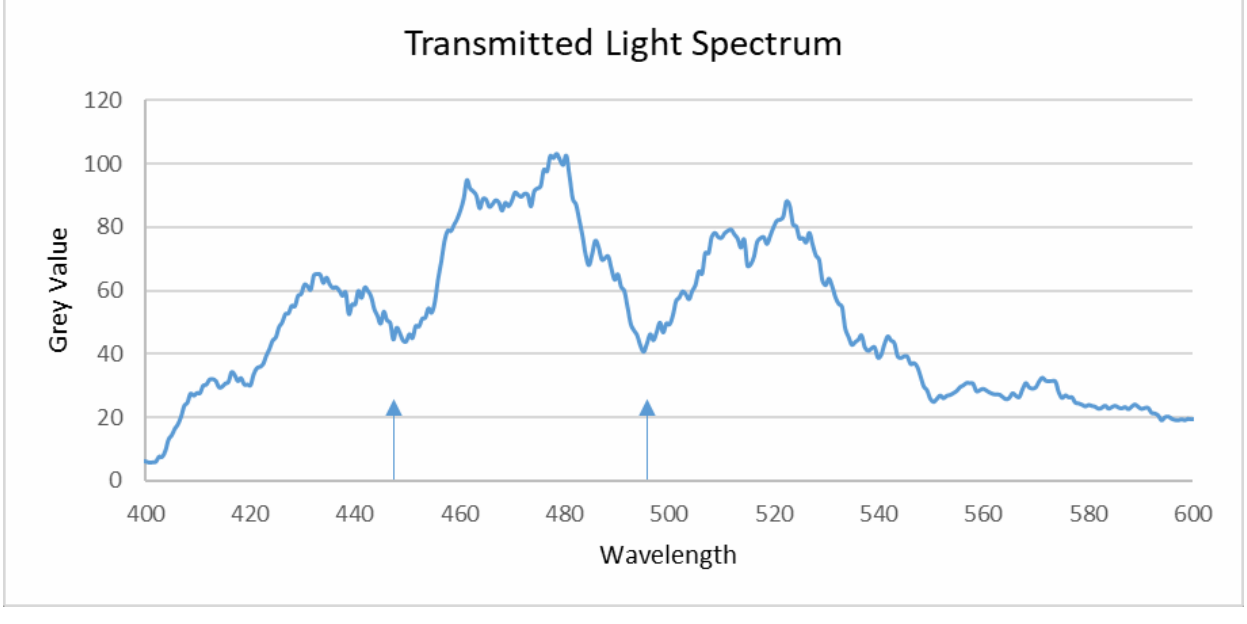

Figure 3.6. The associated wavelength obtained from the coordinate outline in Figure 3.4. Arrows pointing to the valleys are used in size calculation, each at 449.75 and 495.11 nm, respectively.

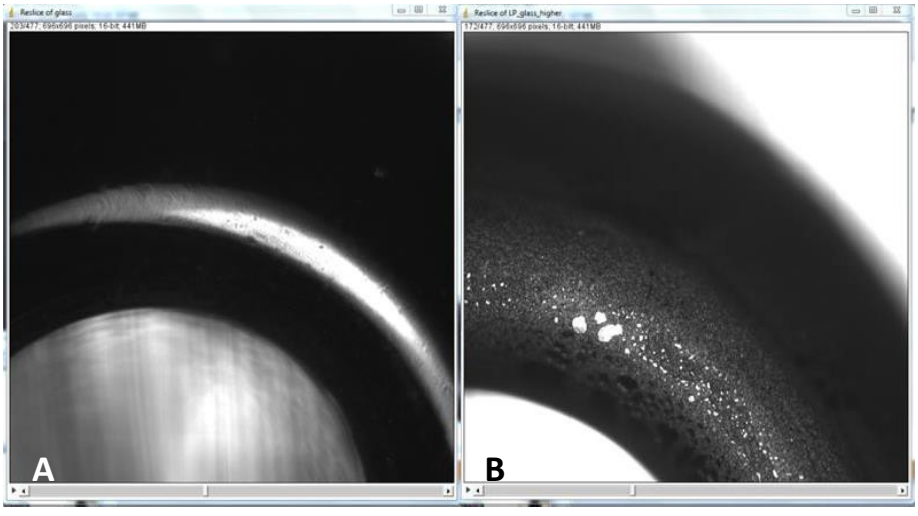

Figure 3.7. Glass seed beads (A) without spores and (B) with spores coating the surface.

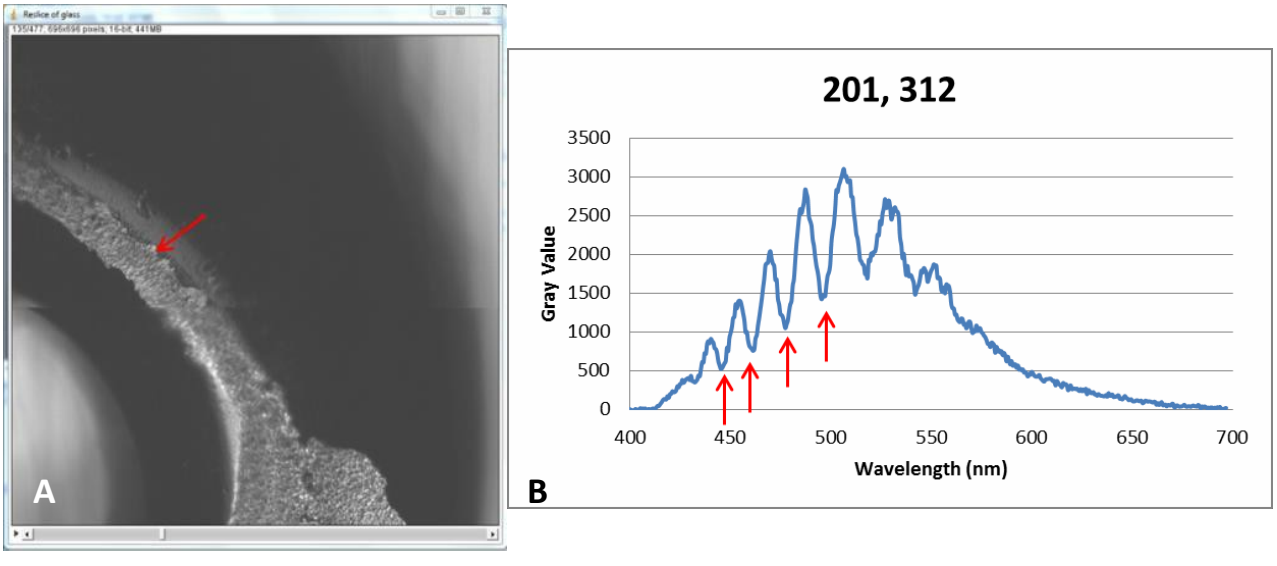

Figure 3.8. (A) A black glass seed bead spore loaded with *Grosmannia alacris* spores and a point associated with (B) the wavelength obtained for sizing, with red arrows denoting minima used in size determination.

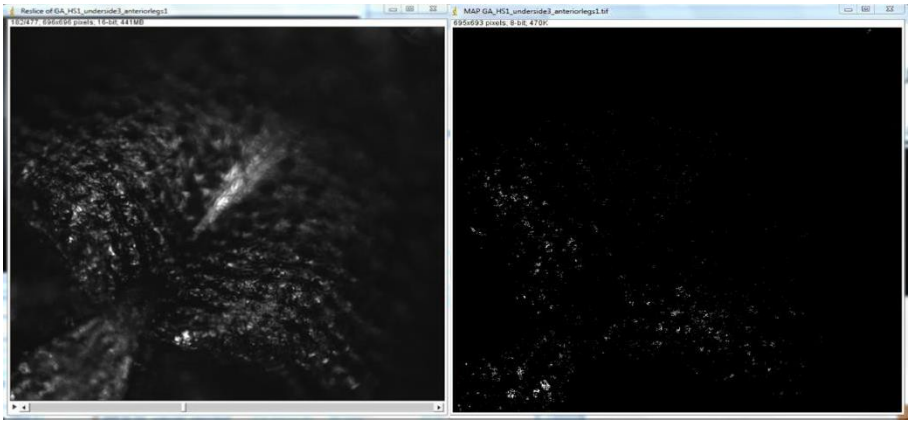

Figure 3.9. (A) An elytral surface of a *H. salebrosus* beetle rolled in spores and (B) regions identified as potential spore locations according to the FFT map code.

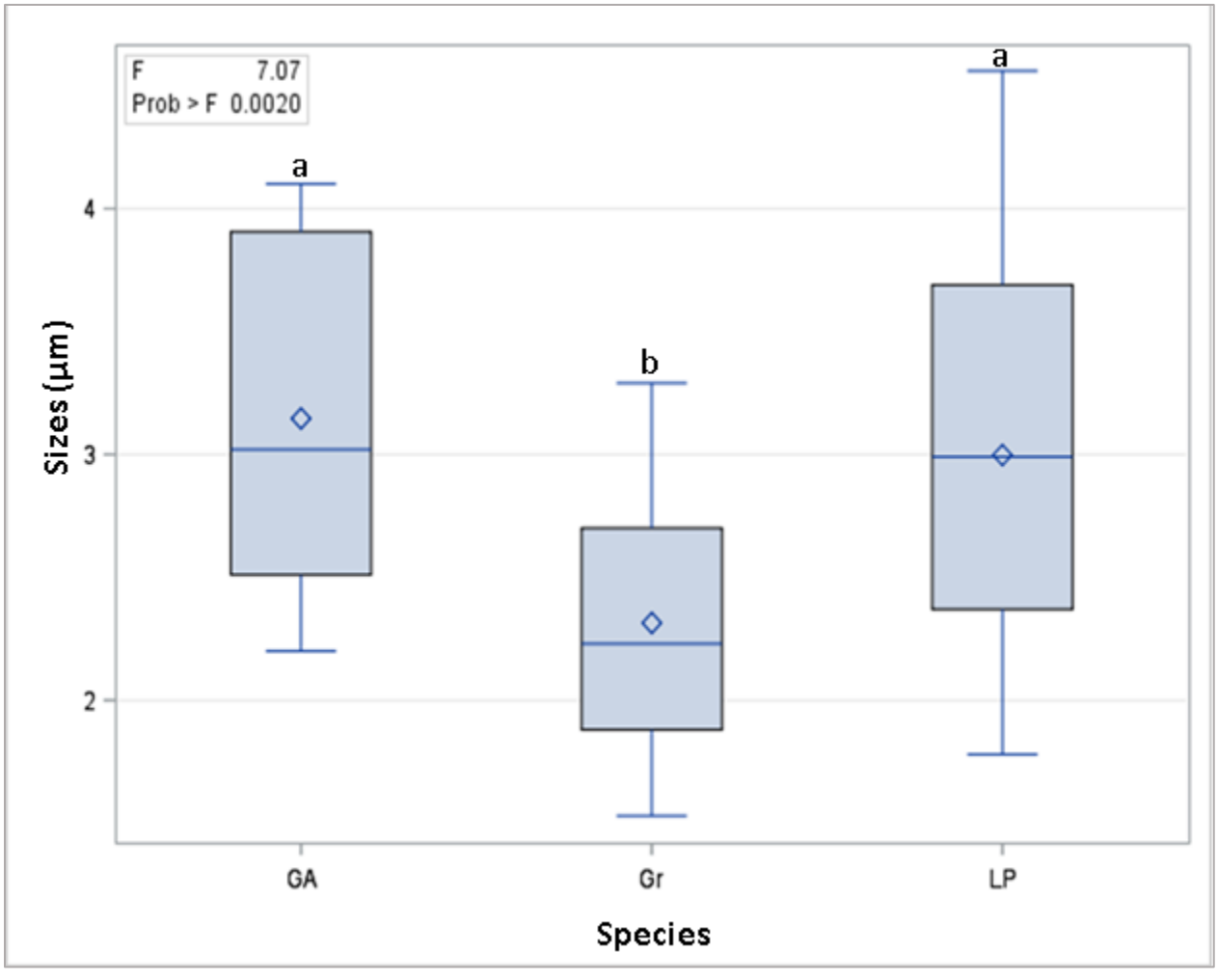

Figure 3.10. Maximum, average, and minimum sizes for each *Grosmannia alacris* (GA), *Graphium* sp. (Gr), and *Leptographium procerum* (LP), where means associated with a different lowercase letter are significant.